

On the Nature of Water Interacting with Brønsted Acidic Sites. Ab Initio Molecular Dynamics Study of Hydrated HSAPO-34

Yannick Jeanvoine and János G. Ángyán*

Laboratoire de Chimie Théorique, UMR CNRS No. 7565, Institut Nancéen de Chimie Moléculaire, Université Henri Poincaré, B.P. 239, 54506 Vandœuvre-lès-Nancy, France

Georg Kresse and Jürgen Hafner

Institut für Theoretische Physik, Technische Universität Wien, Wiedner Hauptstrasse 8-10, A-1040, Wien, Austria

Received: March 27, 1998; In Final Form: June 24, 1998

Recent neutron-diffraction experiments revealed the presence of hydroxonium ions in the hydrated HSAPO-34, an aluminophosphate type zeolitic material, structurally isotypic with chabazite. Ab initio molecular dynamics (AIMD) simulations were used to decide whether the proton transfer from a Brønsted acid site to a single water molecule is possible in this material, or the simultaneous presence of two water molecules in the zeolite cage is necessary to realize such a transfer. The molecular dynamics calculations support the view that while the intrinsic acidity of the Brønsted site in HSAPO-34 is insufficient to protonate an isolated water molecule, the basicity of a hydrogen-bonded water dimer is high enough to act as proton acceptor at the acid site.

1. Introduction

Recent experimental studies, combining infrared spectroscopy and neutron diffraction on a synthetic zeolitic catalyst of aluminophosphate type, HSAPO-34,¹ provided some pieces of evidence that Brønsted acid sites can protonate intrazeolitic water molecules leading to the formation of hydroxonium ions (H_3O^+). The same experiments indicated the simultaneous presence of water molecules hydrogen-bonded to Brønsted acid sites without the formation of ion pair.

Most of the experimental techniques fail to provide an unambiguous proof for the existence of H_3O^+ species in zeolites. The infrared bands attributed by several authors to H_3O^{+2} can also be interpreted in terms of a water molecule H-bonded to an acidic hydroxyl.^{3,4} The assignment of low-temperature broad-line ^1H NMR spectra,^{5,6} or of the ^1H MAS NMR data,⁷ to protonated water species seems to be controversial too. According to a recent analysis, inelastic neutron scattering data for the water molecule in H-ZSM-5 were found to be incompatible with the hypothesis of forming hydroxonium ions in this material, but they could be explained by the hypothesis of a H-bonded complex.⁸

On the basis of theoretical calculations it seems that the proton-transferred complex between a Brønsted site of the zeolite and a single water molecule is not a minimum of the potential energy surface.⁹ This has been concluded from the study of prototype systems which model the complex between the acid site and the water, without¹⁰ or with¹¹ embedding, as well as from calculations on fully periodic hydrated zeolite models.¹² However, recent ab initio studies by the MP2 approach¹⁰ and by Car-Parrinello type DFT calculations¹² showed that the probability of proton transfer might be considerably enhanced at higher water coverages.

The main question is whether the average neutron-diffraction structures should be interpreted by supposing the existence of H_3O^+ species stabilized by the electrostatic field of the zeolite and by H bonds to the framework oxygens, or the proton transfer needs to be assisted by the formation of water dimers leading to H_5O_2^+ species. In order to elucidate the conditions which explain the water protonation in HSAPO-34, observed in neutron diffraction experiments, ab initio molecular dynamics simulations and geometry optimizations were performed on this system.

2. Methods

The calculations were done with the Vienna Ab initio Simulation Package (VASP).^{13,14} The density functional was parametrized in the local-density approximation (LDA), with the exchange-correlation functional proposed by Perdew and Zunger¹⁵ and corrected for nonlocality in the generalized gradient approximation (GGA) using the formulation of Perdew and Wang.¹⁶ The Kohn–Sham equations were solved variationally on a plane-wave basis set with an efficient iterative algorithm, based on the minimization of the norm of the residual vector of each eigenstate and on an effective charge-density mixing. The electron–core interactions were described by ultrasoft pseudopotentials,^{17,18} which allow to use a relatively low value of the plane wave cutoff (300 eV for oxygen).

Molecular dynamics runs were conducted in the microcanonical ensemble, using the Verlet velocity algorithm with $\Delta t = 0.5$ fs. This relatively large time step is justified, since the simulations were performed on deuterated samples, corresponding to the experimental conditions of the neutron diffraction measurements.¹ The simulation temperature (around 300 K) was chosen significantly higher than the experimental one (15 K), in order to allow the system to explore larger regions of the phase space during a trajectory of 3 ps (after 2 ps of equilibration).

* Corresponding author.

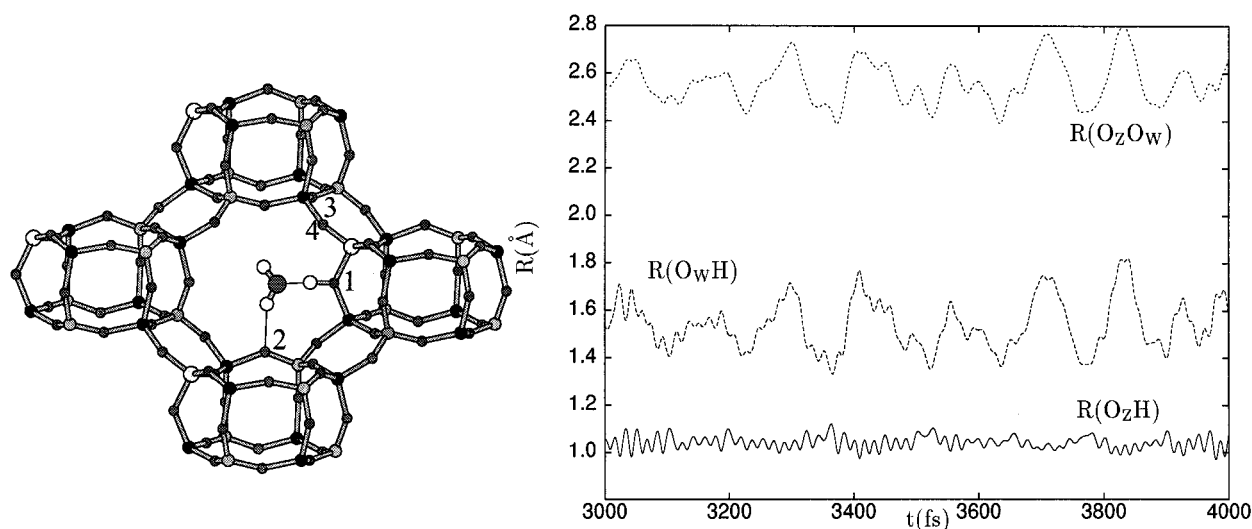


Figure 1. Interatomic distances characterizing the water–acid site complex along a MD trajectory of the monohydrated HSAPO-34·H₂O. Continuous line: $R(\text{O}_z\text{H})$; dotted line: $R(\text{O}_w\text{O}_z)$; broken line: $R(\text{O}_w\text{H})$. The displayed structure is a typical optimized geometry obtained by quenching a point of trajectory.

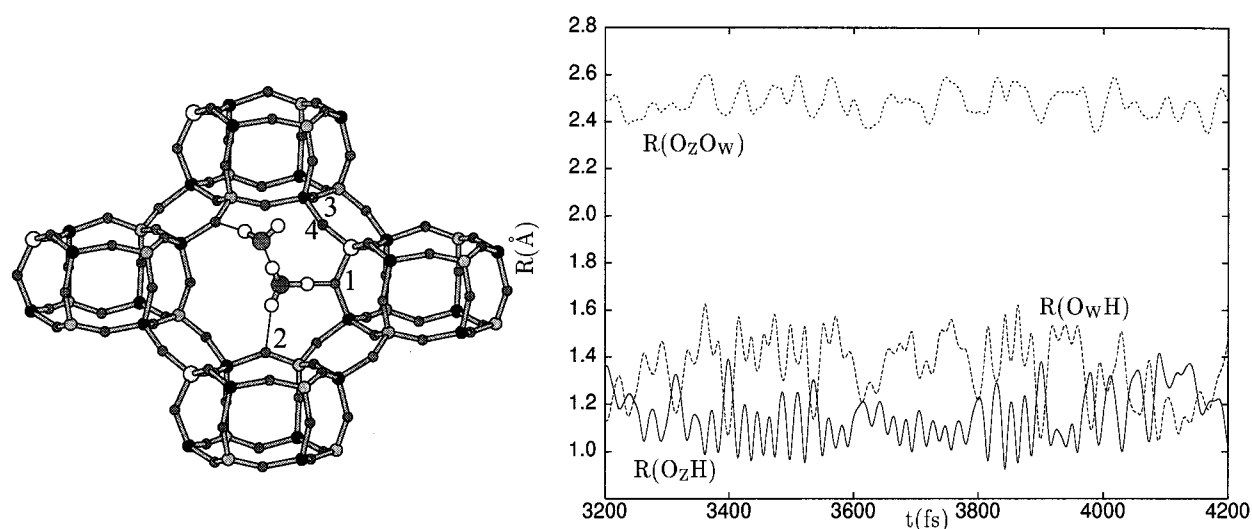


Figure 2. Interatomic distances characterizing the water–acid site complex along a MD trajectory of the dihydrated HSAPO-34·2H₂O. Continuous line: $R(\text{O}_z\text{H})$; dotted line: $R(\text{O}_w\text{O}_z)$; broken line: $R(\text{O}_w\text{H})$. The displayed structure is a typical optimized geometry obtained by quenching a point along the molecular dynamics trajectory.

Structural relaxations, limited to the positional parameters of the atoms, by keeping the cell shape and size fixed at their experimental values (rhombohedral cell, $a = 9.389$, $\alpha = 94.33^\circ$), were performed by a quasi-Newton algorithm, using analytical forces.

3. Results and Discussion

The simulation cell consisted of a primitive unit cell of the SAPO-34 framework, i.e., a hexagonal prism of the tetrahedral atoms. A fragment of the periodic framework structure is illustrated in Figures 1 and 2, showing the four crystallographically distinct oxygen sites. Neutron diffraction data indicate two favorable protonation sites, O(1) and O(2), the former showing a stronger tendency to transfer its proton to a neighboring water molecule.¹

The general composition of the hydrated HSAPO-34 unit cell is $\text{H}_x\text{Si}_x\text{Al}_6\text{P}_6\text{O}_{24} \cdot (\text{H}_2\text{O})_n$. In the case of HSAPO-34, two experimental methods, leading to slightly different values, were used to determine the Si/Al ratio.¹ On the one hand, the fractional occupancy of the phosphorus sites by silicon has been found by MAS NMR to be $x = 1.32$ (Si/Al = 0.22),

corresponding to a net negative charge per unit cell of the silicoaluminophosphate framework equal to $-1.32e$, in good agreement with elemental analysis (Si/Al = 0.19).²

On the other hand, the compensating positive charge deduced from the occupancy of the acid proton (deuterium) sites as obtained by the Rietveld analysis of the neutron data is equal to $2.262e$. MAS NMR estimates of the Si/Al ratio are probably more accurate than the Rietveld occupancy of the proton sites, and therefore it will be assumed that on average there is slightly more than one substitution per unit cell. A quite faithful representation of the experimental facts could have been obtained from a doubled unit cell with three substitutions, corresponding to $x = 1.5$ or Si/Al = 0.25. However, such a model would raise additional complications due to the numerous possible arrangements of three substitution sites in a double cell and would lengthen the simulation times. Therefore, in the following one substitution per unit cell ($x = 1.0$ or Si/Al = 0.16) will be considered.

A first series of simulations was done on the monosubstituted HSAPO-34 model protonated (deuterated) on site O(1) and loaded by one water (D₂O) molecule per unit cell. The number

of water molecules is equivalent to the number of acid protons (deuteriums) in the sample ($n = x$). A typical trajectory, obtained for the monohydrated HSAPO-34 is represented in Figure 1. Three geometrical parameters are plotted: the oxygen–oxygen distance between the water and the Brønsted site, $R(\text{O}_\text{w}\text{O}_\text{z})$; the distance between the zeolite proton and the water oxygen, $R(\text{O}_\text{w}\text{H})$; and the distance OH at the Brønsted site, $R(\text{O}_\text{z}\text{H})$. No tendency of proton transfer can be observed on this trajectory: $R(\text{O}_\text{w}\text{H})$ remains always larger than $R(\text{O}_\text{z}\text{H})$. The acid proton performs a relatively small-amplitude oscillation around its equilibrium position, while the librational amplitude of the loosely bound water molecule is about 0.4 Å.

Geometry optimizations of the monohydrated HSAPO-34 yield systematically H-bonded complexes without proton transfer. As we can see in Figure 1, the water molecule is stabilized with a second H bond formed with the second neighbor of the acid site. This structural feature is usually missed in cluster models, where only first-neighbor oxygens are available to stabilize the complex by the formation of a secondary H bond.¹⁰ However, neither the hydrogen bonds nor the long-range electrostatic effects, fully taken into account in our calculations, are able to stabilize the H_3O^+ ion in the HSAPO-34.

Are these simulations in contradiction with the experimental data¹ of Smith et al.? Not necessarily. Although our monohydrated periodical HSAPO-34 model closely reproduces the average composition, it misses the substitutional disorder of the Si atoms as well as the disorder of protons and water molecules in a real zeolite. Indeed, the distribution of the protonation sites and that of the water molecules is not periodic in a zeolite crystal. The experimentally observed occupancy is a result of an average over domains with various local arrangements of water around possible protonation sites. Among the probable events, one should attribute a privileged role to those where a single Brønsted site interacts with two water molecules. In the framework of a periodic computational model, such events can be represented by a dihydrated HSAPO-34·2H₂O system ($x = 1$, $n = 2$).

The evolution of the three distances characterizing the acid site–water complex, as obtained in molecular dynamics simulations for the dihydrated model, is shown in Figure 2. Differences with respect to the previous trajectory are striking. The amplitude of the water motions becomes considerably smaller (0.22 Å), probably due to the steric hindrance owing to the presence of the second water. In the meantime, the amplitude of the $\text{O}_\text{z}\text{H}$ motion is about 4 times larger than it has been in the monohydrated model and numerous proton jumps can be observed toward the water.

In order to decide whether these proton-transferred geometries correspond to stable structures on the potential energy surface, a series of geometry relaxations were performed starting from several geometries selected along the MD trajectory, satisfying the condition that $R(\text{O}_\text{w}\text{H}) < R(\text{O}_\text{z}\text{H})$. All these relaxations lead to different local minima, some of them losing, others preserving their proton-transferred character (cf. Table 1). The proton-transferred structures are characterized by a small $R(\text{O}_\text{w}\text{O}_\text{z})$ distance, between 2.435 and 2.455 Å, somewhat smaller than the experimentally observed value of 2.51 Å. A typical proton-transferred configuration is illustrated in Figure 2.

The role of the second water molecule remains to be clarified. On the one hand, a part of the free space in the relatively small cavity is occupied by the second water, constraining the first one to remain in the proximity of the acid site. On the other hand, the second water molecule enhances the basicity of the

TABLE 1: Relaxed Geometries Obtained for Some Proton-Transferred Structures Selected along the MD Trajectory of the Dihydrated HSAPO-34^a

	ΔE	$R(\text{O}_\text{z}\text{H})$	$R(\text{O}_\text{w}\text{H})$	$R(\text{O}_\text{w}\text{O}_\text{z})$
HSAPO-34·2H ₂ O	–32.11	1.2460	<u>1.1895</u>	2.4351
	–31.85	1.1649	<u>1.2729</u>	2.4368
	–31.04	<u>1.2364</u>	<u>1.2040</u>	2.4397
	–30.85	1.3206	<u>1.1349</u>	2.4545
	–30.52	<u>1.1282</u>	<u>1.3386</u>	2.4649
	–30.23	<u>1.1017</u>	1.3630	2.4612
HSAPO-34·H ₂ O·CH ₄	–20.24	1.0560	1.4485	2.5018
	–19.53	1.0537	1.4357	2.4861
	–20.53	1.0578	1.4497	2.5030
	–19.03	1.0565	1.4382	2.4913
	–22.03	1.0554	1.4515	2.5023
	–19.90	1.0497	1.4566	2.4988
HSAPO-34·H ₂ O	–18.08	1.0424	1.4783	2.5193
	–19.70	1.0517	1.4554	2.5054
	–18.40	1.0467	1.4661	2.5094
	–19.18	1.0460	1.4663	2.5079
	–19.43	1.0501	1.4387	2.4851
	–17.17	1.0439	1.4879	2.5287

^a Each configuration was quenched into a local minimum. The distances R between the zeolite oxygen (O_z), water oxygen (O_w), and the zeolite proton (H) are also shown. The shorter O–H distance is underlined. For each model we show results for the cases where the second water molecule is removed completely or replaced by a methane molecule and the geometry is relaxed. The interaction energies, ΔE (kcal/mol), of the dihydrated complexes are defined with respect to the energies of the dehydrated HSAPO-34 and of the isolated molecules taking part in the reaction.

proton acceptor water molecule via the formation of a H bond.¹⁹ If we replace the second water by an inert system of similar size, e.g., a methane molecule, and relax again, the geometry of the $\text{O}_\text{z}\cdots\text{H}\cdots\text{O}_\text{w}$ fragment changes completely. The results in Table 1 show that the originally proton-transferred structure rearranges to a H-bonded configuration. In the methane complex the $R(\text{O}_\text{w}\text{O}_\text{z})$ distances increase by about 0.04–0.07 Å with respect to the dihydrated structures and the $R(\text{O}_\text{z}\text{H})$ diminish by 0.05–0.26 Å, while the $R(\text{O}_\text{w}\text{H})$ distances increase considerably, by 0.1–0.3 Å, losing completely the proton-transferred nature of the initial complex. Clearly, a steric confinement effect is not sufficient to assist successfully the proton transfer. The geometrical changes induced by the complete removal of the second molecule from the cavity are very similar to those found in the methane complex (Table 1). We can conclude that the proton transfer is enhanced mainly by the electronic effect of the H bond with the second water molecule, by increasing the basicity of the proton acceptor oxygen atom.

4. Conclusions

Ab initio molecular dynamics simulations of deuterated silicoaluminophosphate, HSAPO-34, containing one and two H₂O molecules per unit cell, showed the primordial importance of forming hydrogen-bonded water dimers. Only such dimers are able to act as efficient proton acceptors to be protonated by the acid site. Geometry optimizations of selected configurations along the trajectory confirmed the possibility of forming stable proton-transferred structures. At variance to the usual hypothesis applied in prototype molecule calculations, the hydroxonium ion (and the water molecule) at the acid site is further stabilized by a secondary H bond with one of the second-neighbor oxygen atoms in the eight-membered ring of the SAPO framework.

The present ab initio calculations, performed on realistic three-dimensional periodic models of an experimentally well characterized zeolitic system, included all the possible factors which may contribute to the stabilization of the hydroxonium ions,²⁰ namely (i) interaction with H₂O species, (ii) multiple H bonds with any of the framework oxygens, and (iii) long-range electrostatic interactions. It has been clarified that neither of these latter factors (ii) and (iii) are able to provide enough stabilization for single H₃O⁺ species. Zeolitic environment seem to promote water protonation via an enhancement of the water basicity through stabilization of H-bonded water dimers. These conclusions may help to identify the most important factors which contribute to the formation and stabilization of protonated hydrocarbons in the initial step of solid acid catalysis.

Acknowledgment. This work has been accomplished in the framework of the GdR Européen "Catalyse Hétérogène". Financial support from the French Ministry of Education, Technology and Research, as well as from the INTAS-RFBR 95-0182 project, is gratefully acknowledged. We thank I.D.R.I.S. (Orsay) for the generously allocated computer time.

References and Notes

- (1) Smith, L.; Cheetham, A. K.; Morris, R. E.; Marchese, L.; Thomas, J. M.; Wright, P. A.; Chen, J. *Science* **1996**, *271*, 799.
- (2) Marchese, L.; Chen, J.; Wright, P. A.; Thomas, J. M. *J. Phys. Chem.* **1993**, *97*, 8109.
- (3) van Santen, R. A.; Kramer, G. J. *Chem. Rev.* **1995**, *95*, 637.
- (4) Pelmenchikov, A. G.; van Santen, R. A. *J. Phys. Chem.* **1993**, *97*, 10678.
- (5) Heeribout, L.; Semmer, V.; Batamack, P.; Dorémieux-Morin, C.; Fraissard, J.; Antos, G. *J. Chem. Soc. Faraday Trans.* **1995**, *91*, 3933.
- (6) Batamack, P.; Dorémieux-Morin, C.; Fraissard, J.; Freude, D. *J. Phys. Chem.* **1991**, *95*, 3790.
- (7) Hunger, M.; Freude, D.; Pfeifer, H. *J. Chem. Soc., Faraday Trans.* **1991**, *87*, 657.
- (8) Jobic, H.; Tuel, A.; Krossner, M.; Sauer, J. *J. Phys. Chem.* **1996**, *100*, 19545.
- (9) Sauer, J.; Ugliengo, P.; Garrone, E.; Saunders, V. R. *Chem. Rev.* **1994**, *94*, 2095.
- (10) Krossner, M.; Sauer, J. *J. Phys. Chem.* **1996**, *100*, 6199.
- (11) Greatbanks, S. P.; Hillier, I. H.; Burton, N. A.; Sherwood, P. J. *Chem. Phys.* **1996**, *105*, 3770.
- (12) Nusterer, E.; Blöchl, P. E.; Schwarz, K. *Chem. Phys. Lett.* **1996**, *253*, 448.
- (13) Kresse, G.; Hafner, J. *Phys. Rev. B* **1993**, *48*, 13115.
- (14) Kresse, G.; Furthmüller, J. *Phys. Rev. B* **1996**, *54*, 11169.
- (15) Perdew, J. P.; Zunger, A. *Phys. Rev. B* **1981**, *23*, 8054.
- (16) Perdew, J. P.; Wang, Y. *Phys. Rev. B* **1986**, *33*, 8800.
- (17) Vanderbilt, D. *Phys. Rev. B* **1990**, *41*, 7892.
- (18) Kresse, G.; Hafner, J. *J. Phys. Condens. Matter* **1994**, *6*, 8245.
- (19) Chipot, C.; Gorb, L. G.; Rivail, J.-L. *J. Phys. Chem.* **1994**, *98*, 1601.
- (20) Sauer, J. *Science* **1996**, *271*, 774.